

Acid Corrosion Inhibition of 1018 Carbon Steel by Using Mentha Spicata

A. Rodriguez-Torres¹, M.G. Valladares-Cisneros², V.M. Salinas-Bravo³, J.G. Gonzalez-Rodriguez^{1,*}

¹ Universidad Autónoma del Estado de Morelos, Centro de Investigaciones en Ingeniería y Ciencias Aplicadas, Ave. Universidad 1001, Chamilpa, C.P. 62209, Cuernavaca, Morelos, México.

² Universidad Autónoma del Estado de Morelos, Facultad de Ciencias Químicas e Ingeniería, Ave. Universidad 1001, Chamilpa, C.P. 62209, Cuernavaca, Morelos, México.

³ Instituto Nacional de Electricidad y Energias Limpias, Av. Reforma 108, Temixco, Mor., Mexico.

*E-mail: ggonzalez@uaem.mx

Received: 24 February 2017 / Accepted: 28 March 2017 / Published: 12 May 2017

A study on the use of *Mentha spicata* (*M. spicata*) as eco-friendly inhibitor for the corrosion of 1018 carbon steel in sulfuric acid was performed with the use of potentiodynamic polarization curves and electrochemical impedance spectroscopy (EIS) measurements at 25, 40 and 60 °C. Results have shown that *M. spicata* is a good, mixed type of corrosion inhibitor. An increase in its efficiency was observed when both its concentration and elapsing time increased, but when the temperature increased, its efficiency decreased. *M. spicata* contains several compounds which contain heteroatoms in their structure, which are chemically adsorbed on to the steel surface by following a Frumkin type of adsorption isotherm, forming protective corrosion products.

Keywords: Acid corrosion, carbon steel, green inhibitor.

1. INTRODUCTION

Acid solutions such as hydrochloric and sulfuric acid, are used in industry for acid cleaning, descaling and pickling steel structures, processes which are commonly accompanied by a substantial metal dissolution [1]. There are many methods used to reduce the corrosion rate in metals, and the use of inhibitors is very popular. Generally speaking, inhibitors used are organic compounds that contain N, O, S hetero-atoms or π -electrons in their molecules. Due to the adsorption on metals surface, a thin layer of protective corrosion products is formed that prevents the diffusion of chemical species which participate in metal ionization; the adsorption of such compounds is carried out by the interaction between the metal and non-participating electrons from hetero-atoms or π -electrons [2] reducing, thus,

the corrosion rate through the increase or decrease of cathodic or anodic reactions [3-6]. However, most of the commercial organic or inorganic inhibitors are toxic, causing a series of environmental issues. Recently much attention has been directed from academic and industrial communities to the study of natural products with low toxicity as green inhibitors of corrosion [7, 8]. Many plants have been proved as corrosion inhibitors in different media such as *Syzygium cumini* [9], *Rhus verniciflua* [10], *Ceratonia siliqua* [11], *Gossipium hirsutum* [12], Black radish [13], *Capsicum frutescens* [14], *Ochrosia oppositifolia* [15], *Garcinia kola* [16], *Phoenix dactylifera* [17] etc.

Antioxidants are molecules capable of retarding the oxidation processes, there are a lot of antioxidant-rich vegetal species, including Lamiaceae family with a great quantity of polyphenolic compounds [18]. *Mentha spicata* is well known as peppermint, which is a plant from the Lamiaceae family, commonly used as flavoring, vegetal medicine and in gastronomy [19-21]. Among its major components are limonene, carvona, β - pineno, 1,8 cineol, β -cariofileno, Germacrene D [22], mentol. Thus, the goal of the present work was orientated to the selective compound extraction by methanol maceration of *Mentha spicata* (*M. spicata*) and study the organic extract as a green corrosion inhibitor in low carbon steel in other aggressive medium (sulfuric acid).

2. MATERIALS AND METHODS

2.1 Vegetal extract preparation

M. spicata was acquired in our university herbal was dried at room temperature ($25^{\circ}\text{C} \pm 4^{\circ}\text{C}$) during a three week time period, and macerated with methanol during 72h. The solvent was filtered and eliminated with a rotary BUCHI evaporator, the organic residual was considered as a natural inhibitor. The obtained solid was used in different concentrations from 0 to 600 ppm in order to estimate the inhibitory activity in corrosion.

2.2 Testing material

Corrosion tests were done with 1018 carbon steel rods, 6 mm in diameter and with a chemical composition of 0.2 % C, 0.6 % Mn, 0.04 % P, 0.003 % Si and balance in Fe. The exposure area for electrochemical tests was 0.3 cm^2 , and for gravimetric was used cylindrical samples of 2.5 cm height. Each specimen surfaces was polished with emery paper down to 600, rinsed and degreased with acetone.

2.3 Aggressive Solution

Analytical grade sulfuric acid, H_2SO_4 , was used to prepare an aggressive solution in a 0.5 M concentration. Different concentrations of *M. spicata* (0 – 600 ppm) were used in order to estimate its corrosion inhibitor activity.

2.4 Electrochemical cell

To carry out the electrochemical tests, a glass conventional cell with three electrodes was used with a silver/silver chloride and a graphite bar as reference electrode and auxiliary electrode respectively. Working electrodes were made of 1018 steel bar with an exposure area of 0.3 cm².

2.5 Polarization curves

Polarization curves were recorded using a Gill potentiostat from ACM Instruments within an interval of -250 to + 250 mV_{SCE}, respect to the free corrosion potential value, E_{corr}, at a scan rate of 1 mV/s. Corrosion current density values were calculated by using Tafel extrapolation [23-25]. The obtained results from the polarization curves were used to obtain inhibitor efficiency values also by using equation 1:

$$\text{I. E. (\%)} = \left[\frac{I_{\text{corr}_1} - I_{\text{corr}_2}}{I_{\text{corr}_1}} \right] \times 100 \quad (1)$$

where I_{corr1} and I_{corr2} are the corrosion current density values without and with inhibitor respectively. EIS measurements carried out with a PC4 300 Gamry potentiostat in a frequency interval 10 KHz to 0.5 Hz at the free corrosion potential value by applying a perturbing signal with amplitude of 10 mV.

2.6 Scanning electronic microscope analysis

Selected specimens from the corrosion tests were observed in a low vacuum LECO Scanning Electron Microscope (SEM)

2.7 FTIR spectroscopic analysis

Extract functional groups were determined by means of infrared spectroscopy in a Bruker machine using KBr tablets. A Bunker Spectroscopy model Tensor 27 was used for this. For the analysis, sample was processed by using anhydrous potassium bromide tablets (KBr).

2.8 Gas chromatography coupled with mass spectrophotometry (GC-MS)

M. spicata methanolic extract was analysed using a Chromatography gas system in a GC 6890 Agilent Plus system, equipped with a capillary column of phenylmethyl-silicone to 5% of 30 cm long and 0.25 mm internal diameter. The device was coupled to an Agilent 5973 Mass selective detector and a Network Mass Identification device (N-15598, Ver. D2.00), in order to identify extract representative biomolecules. Chromatography conditions were from an initial temperature of 45 °C to a final temperature of 250 °C with 10 °C / min temperature gradient.

3. RESULTS AND DISCUSSION

3.1 FTIR characterization

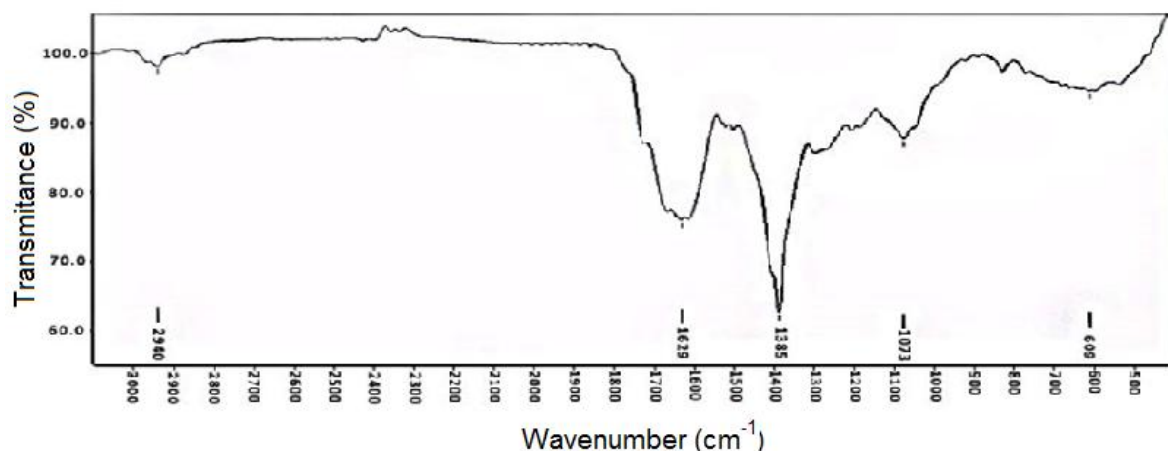


Figure 1. FTIR spectrum of *M. spicata* extract.

M. spicata extract characterization by means of infrared spectroscopy is shown in Fig. 1. The functional groups present in the most abundant compounds of the inhibitor were detected and identified through vibration frequencies in the formed links. The signals appreciated in the spectrum correspond to an alkane as a bond (2940cm^{-1}), C=O double-bond stretching, carboxyl groups and esters (1629cm^{-1}). P-O bond asymmetric stretching in phosphate group and C-H bonds formation (1385cm^{-1}) and typical vibration of C-O bonds of phenolic compounds (1073cm^{-1}) observed in the vibration signal for a simple C-O link, with both signals the presence of functional groups ester type and carboxylic acid were evident in the present compounds of the inhibitor [26].

3.2 Gas chromatography/mass spectrometry (GC-MS)

Table 1. Phytocomponents detected in *M. spicata* extract.

Compound (% of abundance, identification)	Retention time (min)	Molecular ion mass	Fragmentation MS
1-metil-4-(1-metiletil)- Benceno (cimeno) (1.24 %, 10)	7.24	134	119, 91, 77, 65, 51, 27
D-Limoneno (0.77 %, 1)	7.30	136	121, 107, 93, 79, 68, 53, 41, 27
2,3-dihidro-3,5-dihidroxi-6- metil- 4H-Piran-4-ona (1.97 %, 11)	9.18	144	126, 115, 101, 72, 55, 43
5-(hidroximetil)- 2- Furancarboxaldehyde (21.3 %, 12)	10.45	126	109, 97, 81, 69, 53, 41, 29
DL-Norleucine (2.12 %, 13)	12.28	129	56, 72, 56, 43, 30

3,7,11,15-Tetramethyl-2-hexadecen-1-ol (3.11 %, 14)	17.77	278	193, 179, 137, 123, 109, 95, 43
Hexadecanoic acid, methyl ester (1.31 %, 15)	18.64	270	239, 227, 213, 199, 185, 171, 157, 143, 129, 115, 97, 87, 74, 55, 43
Hexadecanoic acid (palmitic acid, 18.92%, 16)	19.04	256	227, 213, 199, 185, 171, 157, 143, 129, 115, 97, 83, 73, 60, 43
Phytol (1.16 %, 17)	20.48	278	196, 23, 111, 95, 81, 71, 57, 43
9-Octadecenoic acid (oleic acid, 15.59 %, 18)	20.73	282	264, 111, 97, 83, 59, 55, 41, 29
Octadecanoic acid (stearic acid, 2.81 %, , 19)	20.91	284	255, 241, 227, 213, 199, 185, 171, 157, 143, 129, 83, 69, 43
1,4,6-Androstan-3,17-dione (6.83 %, 20)	23.03	282	267, 254, 239, 211, 131, 122, 110, 95, 77, 41
Sitosterol (5.77 %, 21)	37.24	414	396, 381, 354, 329, 303, 289, 273, 255, 231, 213, 199, 161, 145, 119, 81, 69, 55, 43, 29

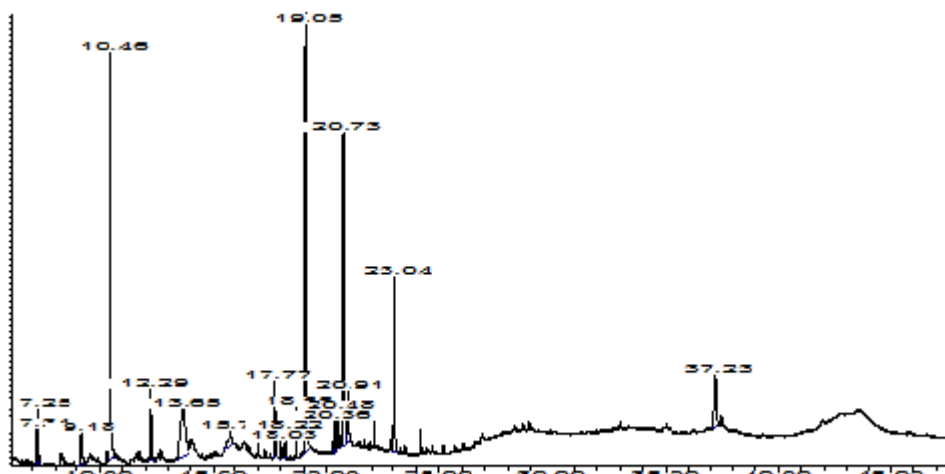
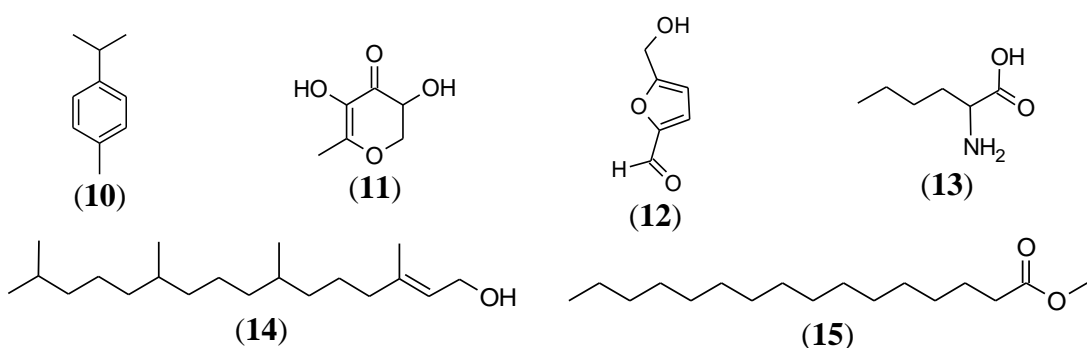


Figure 2. GC-MS Chromatogram of the *M. spicata* extract.



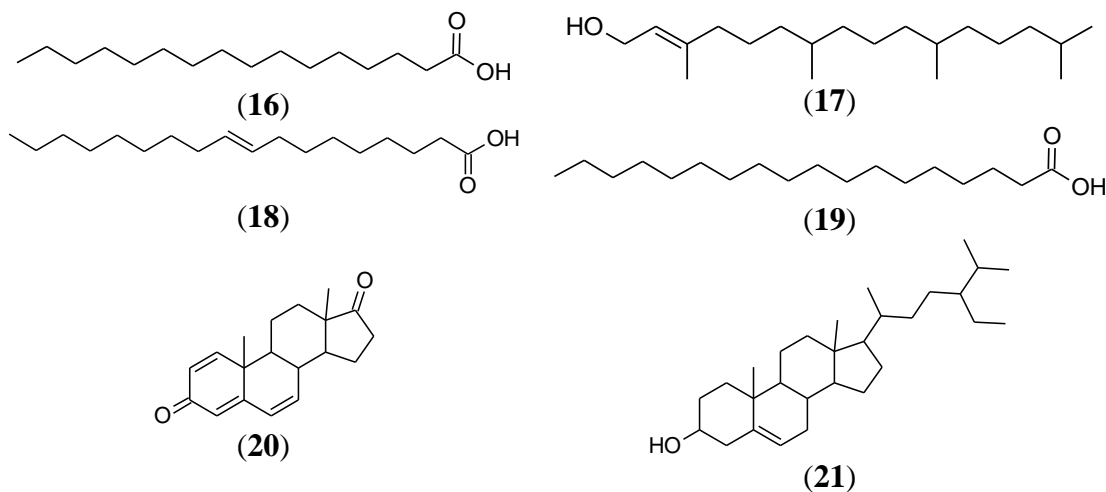


Figure 3. Compounds identified by GC-MS of the methanolic extract of *M. spicata*.

The GC-MS analysis showed that the *M. spicata* extract was formed by thirteen different compounds (table 1, Figs. 2 and 3). The most abundant compounds were 5-(hydroxymethyl)-2-Furancarboxaldehyde, (21.3%), Hexadecanoic acid (18.92 %), 9-Octadecenoic acid (15.59 %), the 1,4,6-Androstatrien-3,17-dione (6.83 %), Sitosterol (5.77 %), 3,7,11,15-Tetramethyl-2-hexadecen-1-ol (3.11 %) and Octadecanoic acid (2.81 %) and DL-Norleucine (2.12 %). The rest of the compounds had a relative abundancy lower than 2%, therefore they are not mentioned. The most abundant compounds are 5-(hydroxymethyl)-2-furancarboxaldehyde, hexadecanoic acid and octadecenoic acid, there are two liquids fatty acids with some polarity, so they have some little solubility in aqueous face.

Some of the major compounds identified in the extract of *M. spicata* have previously been isolated in other plant species, as in the case of 5- (hydroxymethyl) -2-Furancarboxaldehyde. This was the most abundant compound in the extract of *M. spicata* (21.3% from the total), and it was previously identified in *Iphigenia stellata*, vegetable member of terrestrial lilies and belonging to the Colchicaceae family [27]. The found compound contain in their structure □□type double bonds, oxygen as heteroatom and aldehyde functional groups and hydroxyl type, both functional groups containing oxygen, and this heteroatom presents free electron pairs. The other major compounds of *M. spicata* extract were fatty acids: hexadecanoic acid, 9-octadecenoic acid and octadecanoic acid which represent about 28% of the extract. These fatty acids have been previously studied and reported as corrosion inhibitors. Leite et al. reported that gum exuding *Daniella oliverri* inhibited by 72% the corrosion of mild steel in 1.0 M hydrochloric acid, also mentioning that the gum contains 11.73% of hexadecanoic acid [27]. In the study of gum *Gloriosa superbasa* as corrosion inhibitor for aluminium in sulfuric acid, it was reported that among its chemical components, the main component was octadecenoic acid-9 [28]. Checking the inhibitory activity of essential oil of chamomile in the process of corrosion for steel in 0.1 M hydrochloric acid, it was reported that among the active ingredients, it is oleic acid, with a relative abundance of 23.5%, which is the common name given the octadecanoic acid [30]. As these are the major compounds present in the extract, it can be considered as responsible for the possible inhibitory activity in the *M. spicata* corrosion of carbon steel 1018 in H₂SO₄.

3.3 Potentiodynamic polarization curves

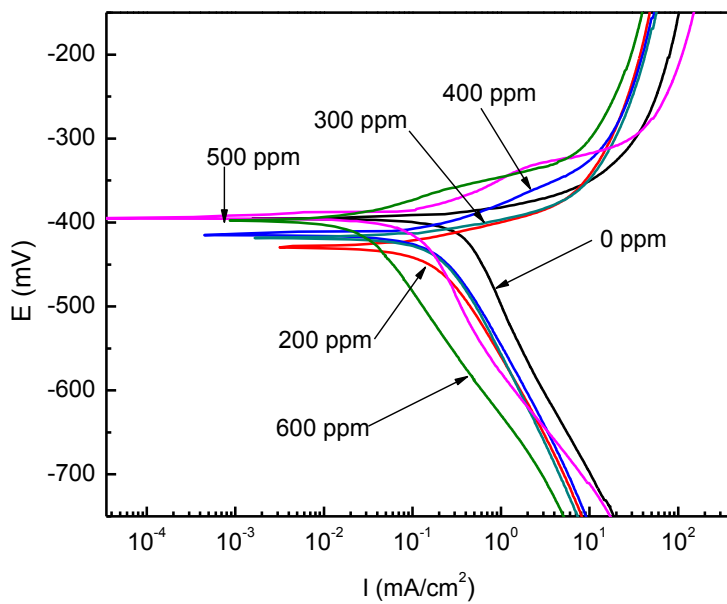


Figure 4. Effect of *M. spicata* concentration on polarization curves for 1018 carbon steel in 0.5 M H_2SO_4 at 25°C .

Fig. 4 shows the polarization curves for 1018 steel in 0.5 M of H_2SO_4 with the addition of different concentrations (0-600 ppm) of *M. spicata* methanolic extract; it is observed the absence of a passive behavior, and that with an increase in the concentration extract, the corrosion current density value decreases; in addition to this, there is a decrease in both anodic and cathodic corrosion density values, which means that the extract affect the oxygen reduction and hydrogen evolution reaction as well as steel oxidation indicating the properties of a mixed type inhibitor [27, 28].

Table 2. Electrochemical parameters obtained from polarization curves for 1018 carbon steel in 0.5 M H_2SO_4 in presence of different concentrations of *M. spicata* at 25°C .

C_{inh} (ppm)	$-E_{\text{corr}}$ (mV _{SCE})	I_{corr} (mA/cm ²)	β_a (mV/dec)	β_c (mV dec)	I.E. (%)	θ
0	393	0.34	34	210	-	-
200	425	0.28	29	203	25	0.25
300	408	0.23	19	206	32	0.32
400	416	0.19	16	201	44	0.44
500	393	0.09	15	153	73	0.73
600	373	0.04	13	116	88	0.88

Electrochemical parameters obtained from these curves are shown in table 2, which shows that the E_{corr} value shifts towards more active values as the inhibitor concentration increases, except at 500 and 600 ppm, where the E_{corr} value was either equal or nobler than that obtained for the uninhibited solution. Inhibitor efficiency increases with an increase in the *M. spicata* concentration and are in

agreement with efficiency values obtained with some other green inhibitors [10-16]. For instance, Prabakaran et al. reported an efficiency value of 91% for the use of *Rhus verniciflua* for the corrosion of mild steel in 1 M H₂SO₄. Oguzie et al. reported efficiency values around 80% for the use of *Capsicum frutescens* [14], whereas Okafor et al. [16] obtained a highest value of 71% for the use of *Garcinia kola*. Both anodic and cathodic Tafel slopes are lowered with the addition of *M. spicata*, indicating that both anodic and cathodic processes, i.e. iron dissolution and oxygen and proton reduction reactions, are lowered [29], indicating that *M. spicata* is acting as a mixed type of inhibitor. The adsorption of *M. spicata* on the steel surface causes a decrease in the anodic reaction, whereas the control of the cathodic reaction in the solution brings a decrease in the cathodic current density is related to [30]. In table 2, θ is the metal surface covered by the inhibitor, and it is calculated by dividing the inhibitor efficiency by 100. By using these data, it is possible to know the way the inhibitor is adsorbed on to the steel surface by using the different adsorption isotherms.

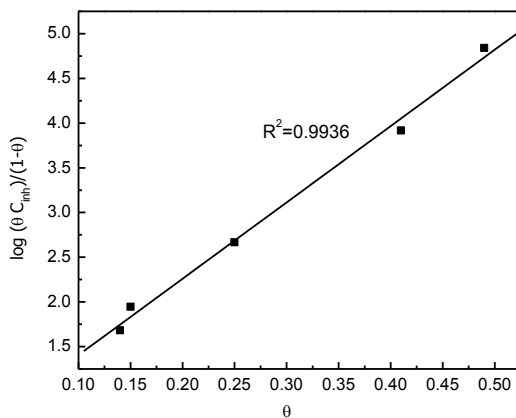


Figure 5. Frumkin adsorption isotherm for 1018 carbon steel in 0.5 M H₂SO₄ in presence of different concentrations of *M. spicata* at 25 °C.

As it can be seen in Fig. 5, the best fit was obtained with the Frumkin adsorption isotherm which is given by:

$$\log \frac{\theta C_{inh}}{1-\theta} = \log K_{ad} + g\theta \quad (2)$$

where K_{ad} is the adsorption-desorption constant and g is an adsorbate interaction constant. By fitting the data, a value of 3.5727 L mg⁻¹ was obtained for K_{ad} , whereas the Gibbs energy, ΔG_{ad} , was calculated by using following equation:

$$\Delta G_{ad}^\circ = -RT \ln K_{ad} \quad (3)$$

obtaining a value of -35.35 kJ mol⁻¹, which is consistent with a chemical type of adsorption.

3.4 Electrochemical impedance spectroscopy (EIS)

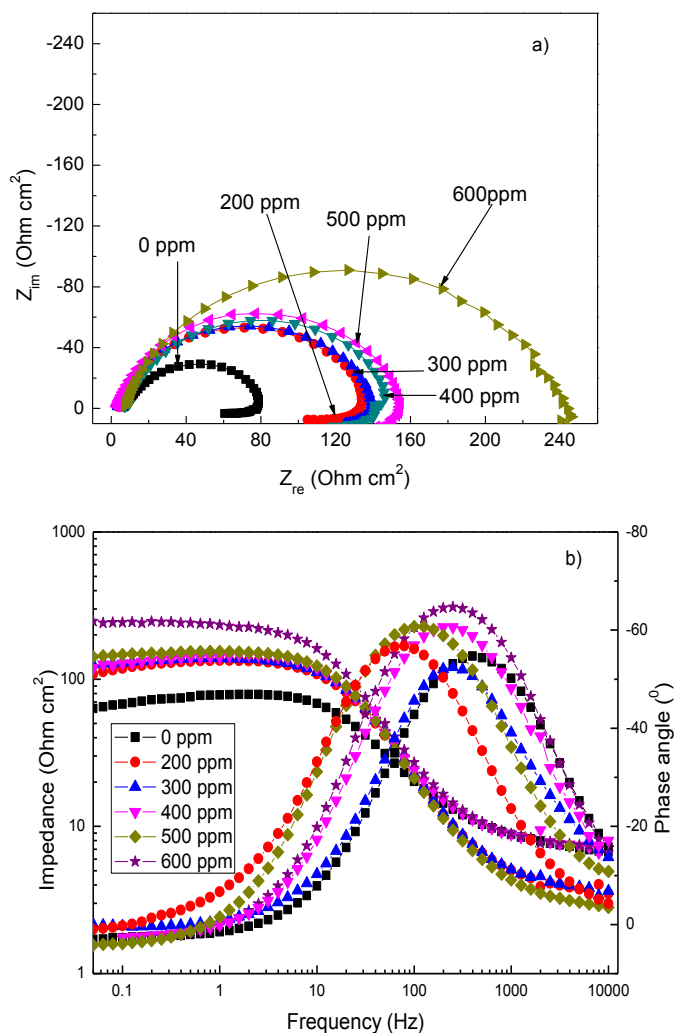


Figure 6. Effect of *M. spicata* concentration on a) Nyquist and b) Bode diagrams for 1018 carbon steel in 0.5 M H_2SO_4 at 25 $^{\circ}\text{C}$.

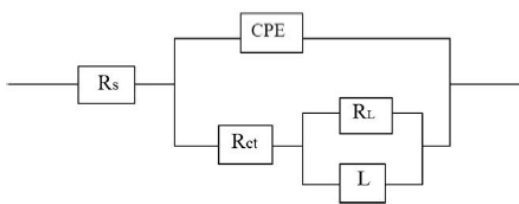


Figure 7. Electric circuit used to simulate EIS data.

EIS data, in both Nyquist and Bode formats for 1018 steel in 0.5 M of H_2SO_4 in presence of different concentrations of *M. spicata* at 25 $^{\circ}\text{C}$ are given in Fig. 6. In the Nyquist diagrams, Fig. 6 a, it is observed at high and intermediate frequencies a depressed, capacitive-like semicircle, whereas at low frequencies an inductive loop can be observed. The first loop is related to the charge transfer resistance, and represents the process occurring at the double electrochemical layer, whereas the

second, inductive loop is related to the adsorption/desorption of intermediate species, maybe aggressive ions, or any kind of formed corrosion products, that cover the metal surface and it indicates that the corrosion process is controlled by the adsorption-desorption of some intermediate species [31]. The charge transfer resistance, which is given by the capacitive loop diameter, increases with increasing the inhibitor concentration, however, perfect loops are not observed due to surface roughness and inhomogeneity [32-34]. This behaviour was similar at all the inhibitor concentrations, which indicates that there is not change in the corrosion mechanism [35, 36]. On the other hand, Bode diagrams, Fig. 6 b, show that the total impedance increases with an increase in the *M. spicata* concentration. Phase angle plots showed a single peak at all inhibitor concentrations, indicating the presence of a single time constant, and the phase angle increased with an increase in the inhibitor concentration up to a value close to -70 degrees.

Thus, studied system could be represented by electric circuit as shown in Fig. 7. In this figure, R_s is the electrolyte resistance, R_{ct} the charge transfer resistance, C_{dl} the double layer capacitance, R_L is the resistance offered to the ions migration in the solution which is manifested in the magnetic fields with their inductance series L that remain dominant within a range of frequencies [37, 38]. However, in practice is very rare to observe an ideal frequency response, and in these cases it is a common practice to employ distributed circuit elements in an equivalent circuit. The most popular way to solve this, is to use elements (CPE) instead of ideal capacitors, which has a non-integer power dependence on the frequency. The impedance of a CPE is described by the expression:

$$Z_{CPE} = Y^{-1} (iw)^{-n} \quad (4)$$

where Y is the admittance, i is $\sqrt{-1}$, w is $2\pi f$, f the frequency and n is a parameter and lies between -1 to 1. To take in to account any surface inhomogeneity such as roughness due to corrosion etc... a CPE is used in a model in place of a capacitor [37-39]. Obtained parameters to simulate EIS data by using electric circuit shown in Fig. 7 are shown in table 3, where it is observed an increase in the charge transfer resistance, R_{ct} , as the inhibitor concentration increases as well as an increase in the inhibitor efficiency obtaining a maximum value of 78 % with 600 ppm of the natural inhibitor.

Table 3. Electrochemical parameters used to simulate EIS data for 1018 carbon steel in 0.5 M H₂SO₄ in presence of different concentrations of *M. spicata* at 25 °C.

C _{inh} (ppm)	R _s (Ohm cm ²)	R _{ct} (Ohm cm ²)	C _{dl} (μF cm ⁻²)	L	n	I.E. (%)
0	6.71	57	92.00	15	0.59	-
200	3.95	133	48.10	22	0.65	57
300	3.23	139	47.00	16	0.69	61
400	8.15	145	45.64	25	0.78	66
500	3.23	153	44.43	14	0.87	70
600	7.43	245	30.21	3	0.93	78

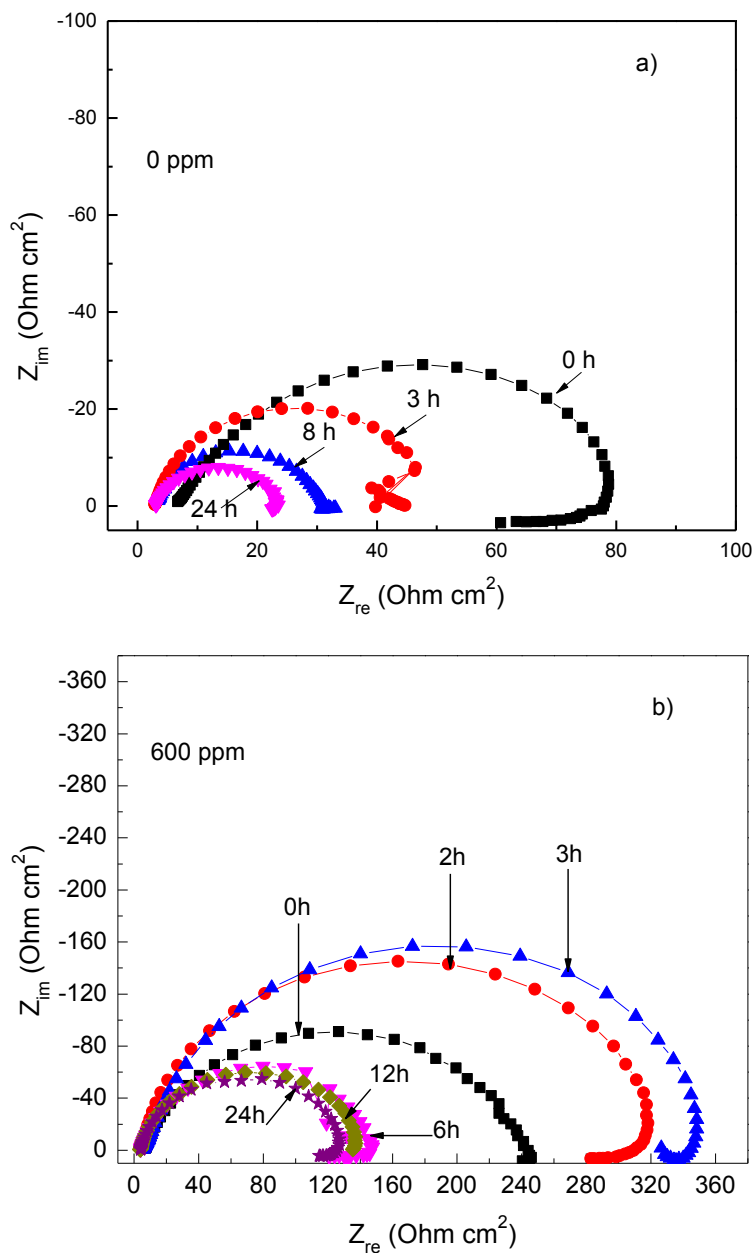


Figure 8. Change of Nyquist diagrams with time for 1018 carbon steel in 0.5 M H_2SO_4 at 25 $^{\circ}\text{C}$ containing a) 0 and b) 600 ppm of *M. spicata*.

The efficiency values obtained by this method are slightly different to those obtained from the polarization curves, but they follow the same trend, maybe due to the fact that in the EIS measurements specimen is polarized only 10 or 15 mV, whereas in the polarization curves specimen is polarized from -250 to + 250 mV_{SCE}, respect to the free corrosion potential value, but this difference has been reported with other green inhibitors [10-16]. A decrease in the double layer capacitance can be observed as the *M. spicata* concentration increases, which is due to the water molecules replacement on the steel surface by the inhibitor molecules.

These points suggest that the inhibitor has to be adsorbed at the metal-solution interface before it can play any role in the corrosion process. The n_{dl} value was 0.5 for the uninhibited solution and it increases with the *M. spicata* concentration, reaching its highest value of 0.9 with 400 ppm of *M. spicata*. When the steel is exposed to the aggressive solution, it will show some degree of roughness, and the n_{dl} value is close to 0.5, but when *M. spicata* is added, the corrosion attack on the steel surface is less pronounced, decreasing this roughness, increasing the n_{dl} value as the inhibitor concentration increases, reaching values close to 1.

In order to elucidate whether *M. spicata* keeps adsorbing on to the steel metal as time elapses, some EIS tests were performed at different exposure times in absence and presence of 600 ppm of *M. spicata*, and the Nyquist diagrams for these tests are presented in Fig. 8. For uninhibited solution, Fig. 8 a, it can be seen that the semicircle diameter of the high frequency capacitive loop, and thus the R_{ct} value, starts to decrease rapidly, which indicates that any corrosion products formed on to the steel surface are desorbed, leaving unprotected the steel, with an increase in the corrosion rate. On the other hand, when the steel is immersed in presence of 600 ppm of *M. spicata*, Fig. 8 b, the semicircle diameter increases up to 3 hours of exposure, with an increase in the R_{ct} value, but after that time, it starts to decrease. The increase in the R_{ct} value, as explained above, is due to the adsorption of *M. spicata*, whereas a decrease in its value indicates desorption from the inhibitor from the steel metal. Inhibitor efficiency values after 3, 8 and 24 hours of exposure were 86, 80 and 79 % respectively, higher than that value obtained at the beginning of the experiment, 78 %, thus, inhibitor efficiency increases with the exposure time.

3.5 SEM micrographs

Fig. 9 shows the micrographs of the corroded surface of 1018 steel samples in 0.5 M H₂SO₄ in presence and absence of 600 ppm of *M. spicata* at different temperatures in the weight loss tests. Figs. 9 a, c and d show the corrosion products on top of specimens without inhibitor at 25, 40 and 60 °C, with the absence of inhibitor after 4 h where it can be seen that corrosion products show defects such as micro cracks and porous, showing the non-protective nature of them. The increment of temperature produces damage on metal surfaces because increases the number of micro cracks and porous and the rate corrosion. On the other hand, for the specimen corroded at 25 °C in presence of 600 ppm of *M. spicata*, Fig. 9 b, the damage is minimum, whereas as the temperature increases, Figs. 9 d and f, the corrosion damage increases, but the corrosion products are more compact and with much less defects than those found in the uninhibited solution at the same temperatures, which indicates that decrease in the corrosion rate is due to the corrosion products formed by *M. spicata* and iron.

Freshly generated Fe²⁺ ions due to corrosion react with inhibitor, which has replaced the water molecules and has been adsorbed on to the steel surface. Adsorbed inhibitor and Fe²⁺ ions form a complex in form of corrosion products which protects the steel from further corrosion [40].

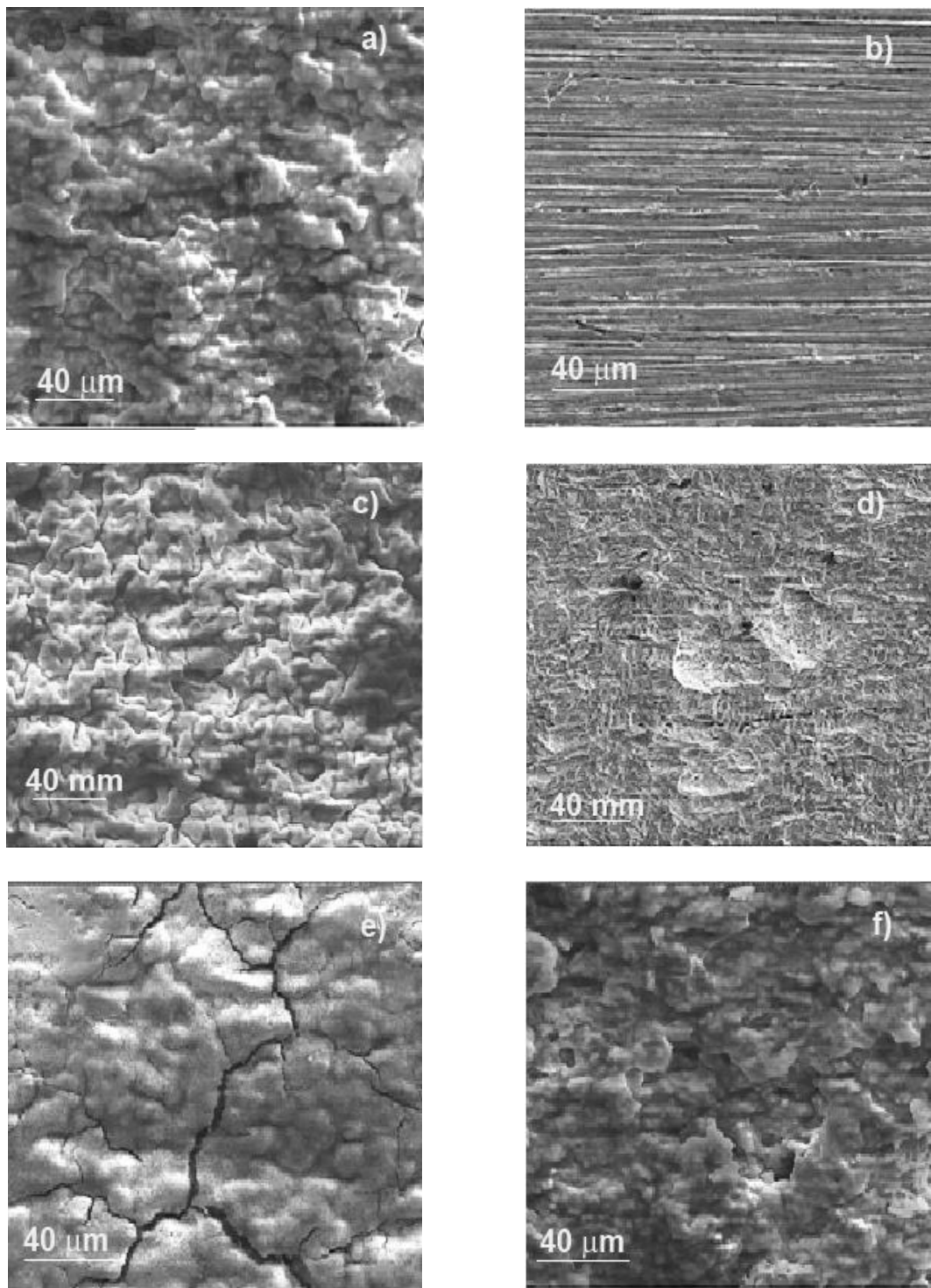


Figure 9. SEM micrographs of 1018 carbon steel samples exposed to 0.5 M H_2SO_4 at 25 (a and b), 40 (c and d) and 60 $^{\circ}\text{C}$ (e and f) containing 0 (a, c and e) and 600 ppm (b, d and f) of *M. spicata*.

As it could be seen from CG/-MS results, *M. spicata* contains several compounds which contain in their structure heteroatoms such as C, N, etc., whose π -electrons can form protective corrosion products by the interaction between the vacant d-orbitals of the iron atom on the metal surface [41]. The adsorption/desorption of this complex is the corrosion process controlling step and

decreases both, the anodic iron dissolution, as well as the cathodic oxygen reduction and hydrogen evolution reactions, decreasing, thus, the corrosion rate.

Table 4. Comparison of the properties of some green corrosion inhibitors with those for *M. spicata*

Green corrosion inhibitor	Inhibitor type	Environment	Metal	Efficiency (%)	Adsorption mechanism	Ref.
<i>Rhus verniciflua</i>	Mixed	1 M H ₂ SO ₄	Mild steel	91	Adsorption of organic molecules	10
<i>Capsicum frutescens</i>	Mixed	0.5 M H ₂ SO ₄	Carbon steel	80	Physical adsorption of molecules	14
<i>Ochrosia oppositifolia</i>	Mixed	1 M HCl	Mild steel	91	Physical adsorption of molecules	15
<i>Garcinia kola</i>	----	0.5 M H ₂ SO ₄	Mild steel	71	Physical adsorption of molecules	16
<i>Carboxymethyl cellulose</i>	----	1 M H ₂ SO ₄	Mild steel	61	Physical adsorption of molecules	42
<i>Safranine-o</i>	Cathodic	1 M H ₂ SO ₄	Mild steel	65	Physical adsorption of barrier layer at interface	43
<i>Bamboo leaf</i>	Mixed	0.5 M H ₂ SO ₄	Cold rolled steel	79	Physical and chemical adsorption	44
<i>M. spicata</i>	Mixed	0.5 M H ₂ SO ₄	Carbon steel	88	Adsorption of the molecules	This work

Table 4 shows a comparison between the properties of some green corrosion inhibitors for mild and carbon steel in sulfuric acid reported in the literature with the performance of *M. spicata* from this work. It can be seen that in most of the cases, tested inhibitors affected both anodic and cathodic reactions, thus, behaving as a mixed type of inhibitor. Also, the inhibitor efficiency value reported for *M. spicata* is in agreement with those reported in the literature, and, even more, they follow the same trend with an increase in the inhibitor concentration or elapsing time. Finally, in all cases it is reported

that in order to protect from the aggressive environment, green inhibitor needs to be adsorbed onto the steel surface, either physically or chemically.

4. CONCLUSIONS

A study of the possibility of using *M. spicata* as corrosion inhibitor of 1018 steel in sulfuric acid has shown that it is a good mixed type of inhibitor. In order to protect the steel, *M. spicata* forms protective corrosion products once it is chemically adsorbed on to the steel surface following a Frumkin type of adsorption isotherm. The efficiency of *M. spicata* increases when its concentration and elapsing time are increased, but is decreased with an increase in the temperature. Chemical analysis of *M. spicata* methanol extract indicates that it contains a high number of compounds such as 5-(hydroxymethyl)-2-Furancarboxaldehyde, hexadecanoic acid, 9-octadecenoic acid and octadecanoic acid, which contain in their structure heteroatoms such as C, N and O, which can react with iron to form protective corrosion products.

References

1. E. E. Oguzie, *Corros. Sci.*, 50 (2008) 2993.
2. N. Vaszilcsin, V. Ordodi and A. Borza, *Int. J. Pharmaceutics* 43(2012) 241.
3. G. Ji, S. K. Shukla, P. Dwivedi, S. Sundaram and R. Prakash, *Ind. Eng. Chem. Res.* 50 (2011) 11954.
4. M. Lashgari and A. M. Malek, *Electrochim. Acta* 55 (2010) 5253.
5. F. Bentiss, M. Traisnel and M. Lagrenée, *Corros. Sci.* 42 (2000) 127.
6. I. B. Obot, N. O. Obi-Egbedi, S. A. Umoren and E. E. Ebenso, *Int. J. Electrochem. Sci.* 5 (2010) 994.
7. L. Cai, Q. Fu, R. Shi, Y. Tang, Y. Long, X. He and K. Ghen, *Ind. Eng. Chem. Res.* 53 (2014) 64.
8. D. Hasson, H. Shemer and A. Sher, *Ind. Eng. Chem. Res.* 50 (2011) 7601.
9. Ghulamullah Khan, Kazi Md. Salim Newaz, Wan Jeffrey Basirun, Hapipah Binti Mohd Ali, Fadhil Lafta Faraj and Ghulam Mustafa Khan, *Int. J. Electrochem. Sci.*, 10 (2015) 6120.
10. M. Prabakaran, S. Kim, V. Hemapriya, M. Gopiraman, I. S. Kim and I. Chung, *RSC Advances*, 6 (2016) 57144,
11. A. S. Fouda, K. Shalabi and A. A. Idress, *Green Chemistry Letters and Reviews* 8 (2015) 17.
12. O. K. Abiola, J. O. E. Otaigbe and O. J. Kio, *Corros. Sci.* 51 (2009) 1879.
13. I. Radojčić, K. Berković, S. Kovač and J. Vorkapić-Furač, *Corros. Sci.* 50 (2008) 1498.
14. E. E. Oguzie, K. L. Oguzie, C. O. Akalezi, I. O. Udeze, J. N. Ogbulie and V. O. Njoku, *ACS Sust. Chem. Eng.* 1 (2013) 214.
15. P. B. Raja, M. Fadaeinab, A. K. Qureshi, A. A. Rahim, H. Osman, M. Litaudon and K. Awang, *Ind. Eng. Chem. Res.* 52 (2013) 10582.
16. P. C. Okafor, V. I. Osabor and E. E. Ebenso, *Pigment and Resin Technology* 36 (2007) 299.
17. S. A. Umoren, Z. M. Gasem and I. B. Obot, *Anti-Corrosion Methods and Materials* 62 (2015) 19.
18. M. S. Ali, M. Saleem, W. Ahmad, M. Parvez and R. Yamdagni, *Phytochemistry* 59 (2002), 357.
19. L. Golestan, L. Seyedyousefi H. Kaboosi and H. Safari, *Int. J. Food Sci. Technol.* 51 (2016) 581.
20. L. Moreno, R. Bello, E. Primo-Yúfera and J. Esplugues, *Phytotherapy Research* 16 (2002) 10.
21. G. İşcan, N. Kirimer, M. Kürkcüoğlu, K. H. C. Başer and F. Demirci, *J. Agricultural and Food Chemistry*, 50 (2002) 3943.

22. F. Brahmi, A. Adjaoud, B. Marongiu, D. Falconieri, D. Yalaoui-Guellal, K. Madani and M. Chibane, *J. Essential Oil Research*, 28 (2016) 211.
23. A. de Sousa Barros, S. M. de Moraes, P. A. T. Ferreira, I. G. P. Vieira, A. A. Craveiro, Raquel Oliveira dos Santos Fontenelle and H. A. de Sousa, *Ind. Crops and Products* 76 (2015) 557.
24. N. V. Likhanova, M. A. Domínguez-Aguilar, O. Olivares-Xometl, N. Nava-Entzana, E. Arce and H. Dorantes, *Corros. Sci.* 52 (2010) 2088.
25. S. Omanovic and S. G. Roscoe, *Langmuir* 15 (1999) 8315.
26. M. Essendoubi, D. Toubas, M. Bouzaggou, M.J. Pinon, M.I Manfait and D.G. Sockalingum, *Biochim. Biophys. Acta*, 1747 (2005) 239.
27. H. Gerengi and H. I. Sahin, *Ind. Eng. Chem. Res.*, 51 (2012) 780.
28. A. O. S. Leite, W. S. Araújo, I. C. P. Margarit, A. N. Correia and P. D. Lima-Neto, *J. Brazilian Chem. Soc.*, 16 (2005) 756.
29. P. Kalaiselvi, S. Chellammal, S. Palanichamy and G. Subramanian, *Mater. Chem. Phys.*, 120 (2010) 643.
30. G. Bereket and A. Pinarbasi, *Corros. Eng. Sci. Technol.* 39 (2004) 308.
31. M. A. Ameer and A. M. Fekry, *Int. J. Hydrogen Energy*, 35 (2010) 11387.
32. R. Solmaz, E. Altunbaş and G. Kardaş, *Mater. Chem. Phys.*, 125 (2011) 796.
33. A. Chetouani, A. Aouniti, B. Hammouti, N. Benchat, T. Benhadda and S. Kertit, *Corros. Sci.*, 45 (2003) 1675.
34. M. Behpour, S. M. Ghoreishi, N. Soltani and M. Salavati-Niasari, *Corros. Sci.*, 51 (2009) 1073.
35. A. Ostovari, S. M. Hoseinieh, M. Peikari, S. R. Shadizadeh and S. J. Hashemi, *Corros. Sci.*, 51 (2009) 1935.
36. F. M. Reis, H. G. de Melo and I. Costa, *Electrochim. Acta*, 51 (2006) 1780.
37. E. Poorqasemi, O. Abootalebi, M. Peikari, and F. Haqdar, *Corros. Sci.*, 51 (2009) 1043.
38. T. Poornima, J. Nayak, and A. Nityananda Shetty, *Corros. Sci.*, 53 (2011) 3688.
39. H. Keles, M. Keles, I. Dehri and O. Serindag, *Mater. Chem. Phys.*, 112 (2008) 173.
40. S. Martinez and I. Stern, *Appl. Surf. Sci.*, 199 (2002) 83.
41. I. Ahamad and M.A. Quraishi, *Corros. Sci.*, 52 (2010) 651.
42. I.E. Uwah, P.C. Okafor, V.E. Ebiekpe, *Arabian J. Chem.* 6 (2013) 285.
43. W. Pal Singh, J.O.M. Bockris. Toxicity issues of organic corrosion inhibitors: applications of QSAR model. In: The NACE International Annual Conference and Exposition., Paper No. 225, Department of Chemistry, Texas A &M University, College Station, TX 77843-3255, 2013.
44. Mohammed A. Amin, Mohamed M. Ibrahim. *Corros. Sci.* 53 (211) 873.